AIP | Journal of Applied Physics

Zinc phosphate chain length study under high hydrostatic pressure by Raman spectroscopy

M. Gauvin, F. Dassenoy, C. Minfray, J. M. Martin, G. Montagnac, and B. Reynard

Citation: Journal of Applied Physics **101**, 063505 (2007); doi: 10.1063/1.2710431
View online: http://dx.doi.org/10.1063/1.2710431
View Table of Contents: http://scitation.aip.org/content/aip/journal/jap/101/6?ver=pdfcov
Published by the AIP Publishing

Zinc phosphate chain length study under high hydrostatic pressure by Raman spectroscopy

M. Gauvin,[a] F. Dassenoy, C. Minfray, and J. M. Martin
LTDS, Ecole Centrale de Lyon, UMR 5513, 69134 Ecully, France

G. Montagnac and B. Reynard
LST, Ecole Normale Supérieure de Lyon, UMR 5570, 69364 Lyon, France

(Received 20 December 2006; accepted 11 January 2007; published online 19 March 2007)

The aim of this study is to combine a diamond anvil cell with *in-situ* Raman spectroscopy to simulate and analyze the effect of pure pressure on the length of phosphate chains in an antiwear film formed in a tribological contact. *In-situ* Raman spectra of $Zn_2P_2O_7$ glass, α-$Zn_3(PO_4)_2$, and γ–$Zn_2P_2O_7$ crystals submitted to high hydrostatic pressure up to 20 GPa were recorded. Evolution of Raman spectra as a function of pressure was studied in the characteristic high frequency range of PO_4 tetrahedra molecular resonance ($650-1300\ cm^{-1}$). When exposed to high pressure, the structure of the sample becomes less ordered. Phase transitions in α-$Zn_3(PO_4)_2$ structure are observed during compression from ambient pressure to 3 GPa. The length of the phosphate chains is conserved up to 20 GPa when samples are subjected to hydrostatic pressure. © *2007 American Institute of Physics*. [DOI: 10.1063/1.2710431]

I. INTRODUCTION

Widely used in engine lubricants, zinc dithiophosphate (ZDTP) additive has very good antiwear properties but raises environmental issues. Formulation of optimized environment-friendly additives relies on the understanding of the basic mechanisms that lead to the antiwear property. ZDTP decomposes through friction between two surfaces to form a protective film called a tribofilm, covering the sliding surfaces. The antiwear property of this additive is believed to result from the tribofilm[1] already characterized by many surface analysis techniques such as atomic force microscopy (AFM),[2] nanoindentation,[3,4] x-ray photoelectron spectroscopy (XPS),[5] Auger electron spectroscopy,[6] x-ray absorption near edge structure (XANES),[7,8] extended x-ray absorption fine structure (EXAFS),[9] etc. These techniques give access to morphology, mechanical properties, chemistry, and structure of the antiwear film. When rubbing surfaces are made of steel, the tribofilm is mainly composed of amorphous, mixed zinc/iron polyphosphates. The amount of iron from the metallic substrate reacting with the polyphosphates is controlled by the severity of friction conditions. Tribofilm typical thickness is a few hundred nanometers with pads surrounded by valleys on its surface. Pads are elongated in the sliding direction and can reach a few microns in length. They are thought to be the regions of contact between the sliding surfaces, with the summits bearing the highest loads. Depending on friction conditions, flash pressures and flash temperatures are believed to occur on the top of the antiwear film asperities during friction.[10,11] Flash temperatures are responsible for the ZDTP thermal decomposition that provides precursory compounds necessary to the thermal formation of phosphate chains.[12] Crystals and glasses of polyphosphate are polymer-like structured. PO_4 tetrahedra are the basic units of the phosphate chain. They are bounded to each other via bridging oxygens (O_B). Polyphosphate chains are linked together through the interaction of the metallic cations with the nonbridging oxygens called terminal oxygens (O_T). The length depends on the ratio of the amount of metallic cation to phosphorus ([Zn,Fe]/[P]). In the tribofilm, length of polyphosphates chains is heterogeneous. It contains long chain polyphosphates (metaphosphate) in the immediate superficial layer and shorter chains (pyro-ortho phosphate) downward the metallic substrate.[7,8] Nicholls *et al.*[10] performed high spatial resolution chemical analysis coupled to nanoindentation on pad surfaces and regions between them called valleys. These measurements confirm the presence of long-chain polyphosphates on pad surfaces and short chains with unreacted ZDTP in the valleys and highlight the contrasting elastic properties of the two distinct regions. In accordance with Graham *et al.*,[13] the tops of the pads have a higher elastic modulus than the valleys. Hence, the authors suggested that the high flash pressures experienced on the tops of the pads induce the formation of stiff long-chain polyphosphates, while polyphosphates and ZDTP species in valleys are left soft and short due to the relatively low pressure. To our knowledge, no clear experimental evidences has emerged that sheds light on the effect of pressure on polyphosphate chain length.

Recently, Mosey *et al.*[11] have emphasized in molecular dynamics simulation, the role of zinc as a cross-linking agent between phosphate chains by increasing its coordination number, when zinc phosphates are pressurized in hydrostatic conditions. It appears that the relative increase in density due to the cross-linking action of zinc depends on the maximum pressure experienced by the system. According to the pressure-induced cross-linking theory, the tops of tribofilm pads are stiff compared to the edges because of the higher pressure experienced at their summits. Valleys are even

[a]Author to whom all correspondence should be addressed; electronic mail: melanie.gauvin@ec-lyon.fr

softer since pressures achieved in these regions are relatively low. However, this theory does not explain polyphosphate chain length repartition in the ZDTP tribofilm. Therefore, it is important to examine whether pressure is responsible for phosphate chain length heterogeneities.

Raman spectroscopy is a sensitive probe of phosphate polymerization and structural changes in both crystalline and amorphous solids.[14–22] P-O-P and P-O_T bonds have a distinct vibrational response. Symmetric stretching of P-O_B bonds is active in the 600 to 800 cm^{-1} and P-O_T bonds show a set of resonance between 900 and 1300 cm^{-1}. Belonging to the same phosphate backbone, P-O-P and P-O_T bond vibrations are correlated. In a general way, when chain length decreases, bands in the 600–800 cm^{-1} region shift to higher wavenumbers, and bands in the 900 and 1300 cm^{-1} domain shift to lower wavenumbers at the same time.

Here, we study *in situ* the effect of applied hydrostatic pressure on zinc phosphates using Raman spectroscopy.

II. EXPERIMENT

Commercial zinc orthophosphate powder [$Zn_3(PO_4)_2$, 99.99%] provided by Alfa Aesar, and zinc pyrophosphate powder ($Zn_2P_2O_7$, 99%) supplied by the Budenheim company were used without further purification. Owing to their high hygroscopic properties, phosphates break down in the presence of atmospheric humidity. Thus, powders were heated to 500 °C overnight prior to analysis and stored in dry atmosphere. X-ray diffraction (XRD) analysis were performed from 10° to 80° (2θ) in reflection geometry, using the $K\alpha$ copper radiation at 1.54 Å in order to identify the crystal phase of each sample. After heating, XRD and Raman spectra lines were more intense and better resolved. Products were identified as α-$Zn_3(PO_4)_2$ and γ-$Zn_2P_2O_7$ compounds.[23,24]

The number of bridging oxygen per PO_4 tetrahedra was obtained by ^{31}P liquid-state NMR analysis[17] using a Bruker Avance 250 spectrometer. Spectra were recorded at 101.2 MHz, using a 2.7 μs pulse and 5 s relaxation time with a spinning speed of 20 Hz. Using a high quenching rate from above the melting temperature allows us to obtain a glass from the pyrophosphate composition, but not from the orthophosphate. The glassy structure was confirmed by Raman spectroscopy.

We performed high pressure experiments on the amorphous and crystalline phases. We used a Mao-Bell-type diamond anvil cell equipped with low-fluorescence diamonds. The compression chamber consists of a 150 μm hole drilled in a preindented stainless-steel gasket. In order to avoid any reaction of the sample with an aqueous medium, paraffin oil was used as a pressure transmitting medium. The calibrated R1 fluorescence shift of a ruby chip is the pressure indicator[25] in the chamber. Raman spectra were recorded in the backscattered geometry with a Labram HR800 equipped with a notch filter and a 1800 g mm^{-1} monochromator which achieves a 1 cm^{-1} resolution. Acquisition times were about 200 s. Raman spectra were recorded for a wide range of frequencies from 150 to 1290 cm^{-1}. For the sake of clarity, we only show the high frequency region (650–1290 cm^{-1}) where the characteristic frequencies of phosphate compounds are observed. Higher frequencies cannot be recorded due to the very intense peak of the diamond window[26] at 1332 cm^{-1}. The 514.5 nm excitation wavelength is provided by a Ar^+ laser. For this study, 280 mW were delivered by the laser yielding a few milliwatts on the sample. A microscope is combined to the spectrometer in order to deliver a few microns wide spot on the sample.

III. RESULTS

A. Ambient pressure spectra

The Raman spectra of zinc phosphate samples at ambient pressure are represented in Fig. 1. The amorphous zinc pyrophosphate spectrum displayed on Fig. 1(a) is in good agreement with previous studies.[14,17] Two sets of resonance characterize the Raman spectrum of amorphous zinc pyrophosphate at ambient pressure: from 700 to 800 cm^{-1} with a maximum at 759 cm^{-1} and from 900 to 1300 cm^{-1} with two maxima at 970 and 1045 cm^{-1}. The resonance observed in the 700–800 cm^{-1} region, at 759 cm^{-1} was attributed to symmetric stretching of P-O-P bonds, and 970 and 1045 cm^{-1} peaks were assigned to symmetric stretching of P-O_T.[14]

Figure 1(b) shows the Raman spectrum of γ-$Zn_2P_2O_7$ at ambient pressure. It displays complex sets of resonance consistent with the glass of the corresponding composition spectrum. One can observe two peaks in the 700–800 cm^{-1} range, at 762 and 777 cm^{-1}. From 900 to 1300 cm^{-1}, the spectrum consists of three majors peaks at 1040, 1067, and 1095 cm^{-1} surrounded by much less intense peaks at 955, 1004, 1133, 1186, and 1222 cm^{-1}. Based on α-$Zn_2P_2O_7$ band assignment,[21] 762 and 777 cm^{-1} peaks were attributed to symmetric stretching of P-O-P bonds and peaks located above 1000 cm^{-1} were assigned to P-O_T bond resonance. Assignment of the 955 cm^{-1} weak peak is ambiguous. It could be attributed to the asymmetric stretching of P-O-P bonds,[21] it could also be due to the vibration of P-O_T bonds in orthophosphate type tetrahedra [cf Fig. 1(c)]. NMR analysis revealed the presence of two types of phosphate tetrahedra, the large majority (~84%) consists of dimers of phosphate expected in pyrophosphate composition and a relatively small proportion of isolated tetrahedra of orthophosphate type.

Figure 1(c) shows the Raman spectrum of α-$Zn_3(PO_4)_2$ at ambient pressure. The zinc orthophosphate sample spectrum consists of a well-resolved triplet of peaks at 965, 1008, and 1047 cm^{-1} and a much less intense doublet of peaks at 1158 and 1178 cm^{-1}. Those peaks are attributed to P-O_T bond resonance in isolated PO_4 tetrahedra.[22] It is of note that the Raman spectrum of zinc orthophosphate is not active in the 650–800 cm^{-1} range which confirms the absence of P-O-P linkage in this composition at ambient pressure. In the following section, we will focus on the evolution of these bands of resonance which are characteristic of the polymerization state of phosphate compounds, over the pressure range up to 20 GPa.

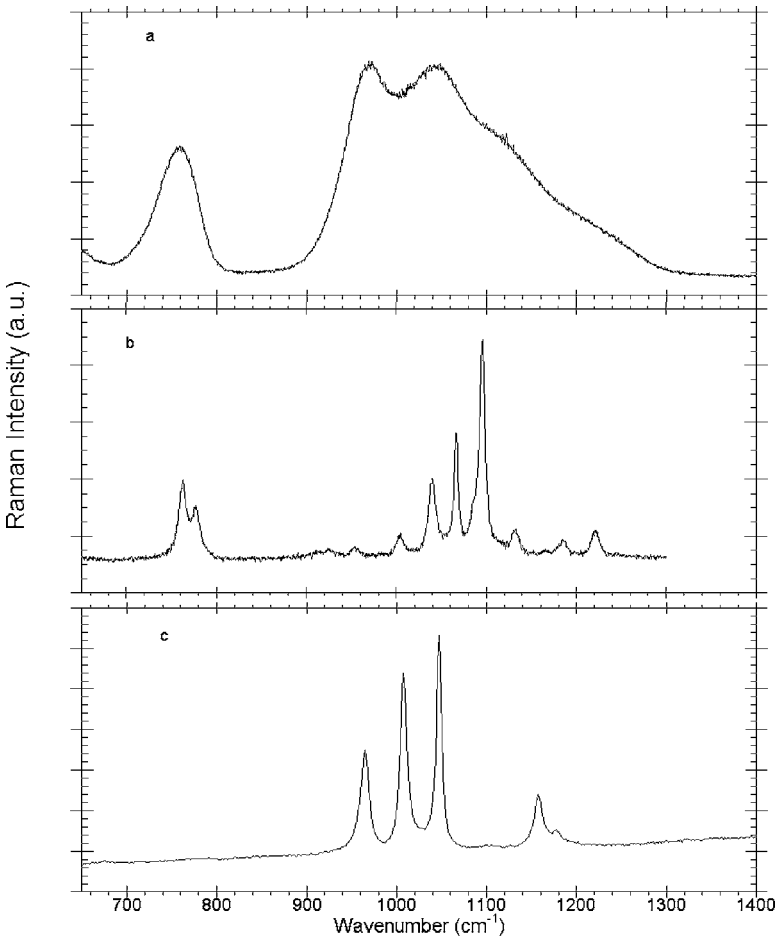

FIG. 1. Raman spectra of zinc phosphates in the 600–1400 cm^{-1} range at ambient pressure. (a) Amorphous zinc pyrophosphate; (b) zinc pyrophosphate crystal; and (c) zinc orthophosphate.

B. High pressure spectra

The Raman spectra of amorphous zinc pyrophosphate up to 21.7 GPa, and decompression are represented in Fig. 2. As the pressure increases, the two regions of interest shift continuously to high wavenumbers. Besides the pressure-induced Raman shift, the 759 cm^{-1} bandwidth starts to increase and the peak height decreases. We also observe a broadening of bands in the 900–1290 cm^{-1} region at ~18 GPa. Evolution of spectra with pressure is continuous, it is thus possible to follow the Raman shift as a function of pressure. Initially positioned at 759 cm^{-1} at 0.1 MPa, the broadened band shifts progressively to end up at 814 cm^{-1} at ~22 GPa, while the 970 and 1045 cm^{-1} peaks at ambient pressure end up at 1014 and 1086 cm^{-1}, respectively, at ~22 GPa. The positive pressure-induced shift corresponds to compression of bonds. This pressure-induced shift is reversible under decompression, except for the 759 cm^{-1} bandwidth which is slightly broader compared to the starting sample. Thus, there is no evidence of emergence or disappearance of the bands of resonance which could testify to the formation of new compounds. The initial chain length of the amorphous pyrophosphate is conserved through the whole pressure range.

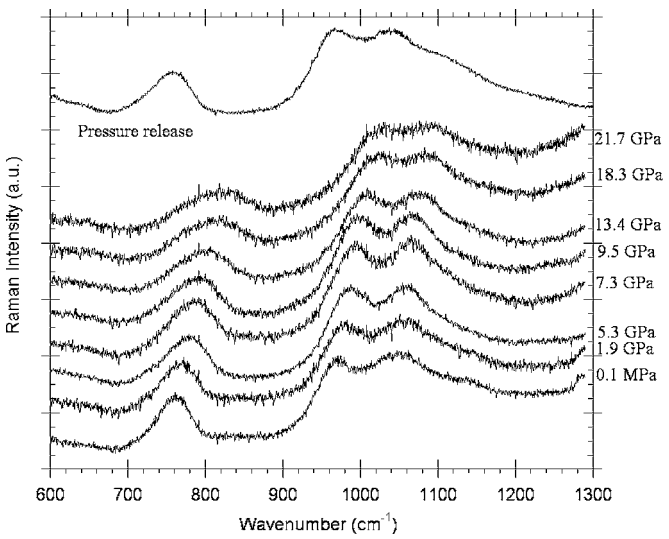

FIG. 2. Raman spectra of zinc pyrophosphate glass in the 600–1290 cm^{-1} range up to 21.7 GPa and after pressure release.

The Raman spectra of crystalline zinc pyrophosphate up to 20 GPa and after decompression are represented on Fig. 3. Up to 3 GPa, ambient pressure Raman features shift continuously to higher wavenumbers. At ~5 GPa, characteristic bands of resonance start to get wider and resolution of the Raman signal decreases. At 9.2 GPa, an ambiguous weak contribution appeared at 729 cm^{-1} and remains up to 18 GPa. This band could be attributed to the resonance of bridging oxygens in metaphosphate chains. However, no associated P-O_T band emerges in the 1200 cm^{-1} region. Hence, there is little probability that this emerging contribution testifies of growing phosphate chains. At 13 GPa, most intense peaks have almost overlapped and shifted to form wide bands

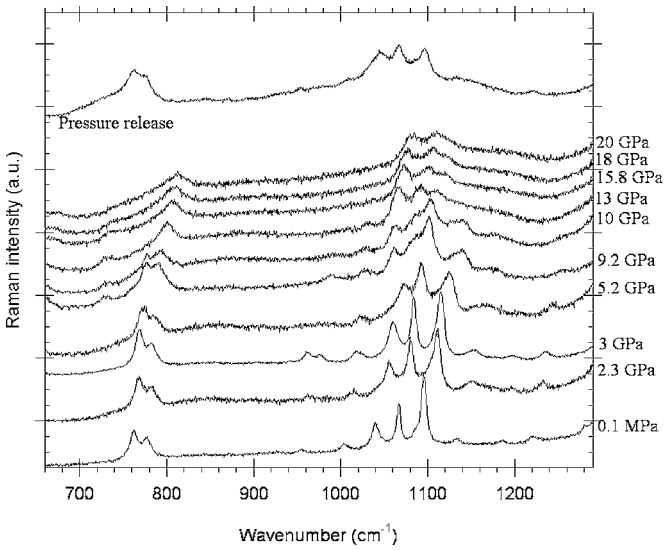

FIG. 3. Raman spectra of zinc pyrophosphate in the 660–1290 cm^{-1} range up to 20 GPa and after pressure release.

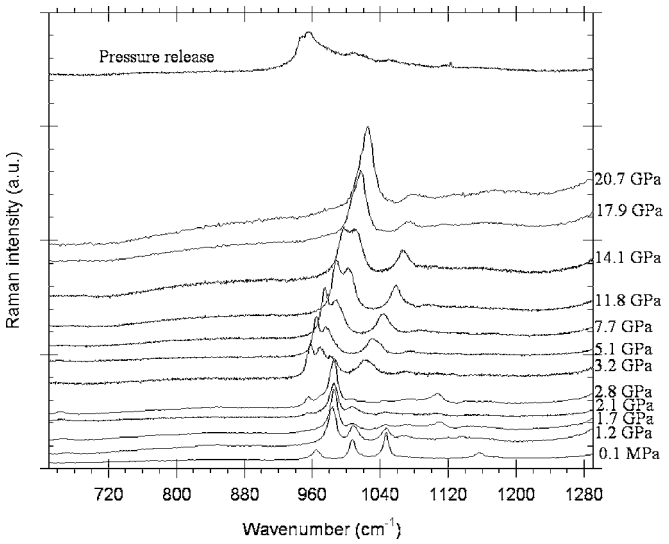

FIG. 4. Raman spectra of zinc orthophosphate in the 650–1290 cm^{-1} range up to 20.7 GPa and after pressure release.

whose maxima are located at 800, 1030, 1066, and 1090 cm^{-1}, while weaker peaks are too broad to be observed. This broadening trend, followed by a positive band shift carries on up to 20 GPa.

These transformations in the Raman spectra imply some loss of crystalline order introduced by the stress field in the chamber at high pressure.[27,28] Broadening and vanishing of low wavenumber bands (not shown) at ~9 GPa support the previous hypothesis. When the pressure is totally released, the transformation is partially reversible. The unloaded sample exhibits maxima of resonance whose positions did not change compared to the original material, except that the initial peak at 1040 cm^{-1} finishes at 1044 cm^{-1}. The sample is partially disordered as confirmed by enlarged bands in the Raman spectrum of the sample. Confirming the evolution of the zinc pyrophosphate glass with pressure, γ-$Zn_2P_2O_7$ does not experience phosphate polymerization leading to a metaphosphate-like structure (i.e., long-chain phosphate). The comparison between the evolution of phosphate chain lengths in the crystal and the glass of corresponding composition is similar. Therefore, we have studied the chain length of a crystalline orthophosphate sample under pressure, which is believed to be analogous to the amorphous orthophosphate that could not be synthesized.

In Fig. 4 one can observe the Raman spectra of crystalline zinc orthophosphate as a function of pressure up to 20.7 GPa, and after decompression. From ambient pressure to 1.2 GPa, the relative intensities of peaks belonging to the triplet invert. An important 19 cm^{-1} shift toward higher wavenumbers and an increase in intensity is observed for the peak initially located at 965 cm^{-1}. The 1008 cm^{-1} peak ends up at 1010 cm^{-1} and the 1047 cm^{-1} peak does not shift. Meanwhile, their intensities strongly decrease. At 1.7 GPa, the spectrum is dominated by a strong peak located at 986 cm^{-1} and two weak bands are observed at 1010 cm^{-1} and the 1047 cm^{-1}. At 2.1 GPa, two contributions at 955 and 971 cm^{-1} appear in the dominant peak shoulder. Between 2.8 and 3.2 GPa a break in the Raman signal occurs where the two latter emerging contributions intensities increase tremendously to form a dominant doublet. A broad peak at 1024 cm^{-1} emerges as well.

At 5.1 GPa, the Raman spectrum of zinc orthophosphate is composed of three major peaks located at 964, 978, and 1030 cm^{-1}. These features shift continuously upon pressurization up to ~14 GPa. At ~14 GPa, peaks belonging to the doublet (997, 1012 cm^{-1}) start to overlap. Meanwhile, bands of resonance in the 200–600 cm^{-1} region (not shown) start to vanish and/or broaden as the pressure increases. At ~18 GPa, the Raman spectrum is dominated by an intense and wide peak located at 1018 cm^{-1} and a much less intense band at 1074 cm^{-1}. The loss of resolution above 14 GPa suggests that the lack of order in the sample is caused by the stress field in the sample chamber at high pressure. This hypothesis is strengthened by the broadening and disappearance of low wavenumber peaks (not shown) with pressure. Upon pressure release the initial structure is not recovered. After decompression the sample is irreversibly disordered, yielding a broad spectrum similar to the amorphous orthophosphate Raman spectrum published in the literature.[17] Zinc orthophosphate experiences pressure-induced phase transitions at relatively low pressure (1–3.2 GPa). Over this pressure range, the sample seems to adopt a higher symmetry structure as suggested by the single peak dominating the spectrum. Although interpretation of the $Zn_3(PO_4)_2$ phase transition is beyond the scope of this study, we should mention that high pressure phase transitions in the orthophosphate compounds[27,29] ($AlPO_4$ and $GaPO_4$) have been observed and attributed to the cation coordination number increase. Besides, no band of resonance emerges in the 650–800 cm^{-1} domain corresponding to P-O-P bond resonance during this experiment. Figure 4 suggests that pressure affects the immediate environment of the orthophosphate but such modifications do not increase the length of phosphate chains by means of P-O-P bond formation.

IV. DISCUSSION

The tribofilm formed through ZDTP decomposition is rather amorphous. In this study, only short-chain zinc pyrophosphate glass was synthesized and no polymerization of phosphate tetrahedra was observed in the amorphous structure when pressurized up to 21.7 GPa. Similarly, compression up to 20 GPa of the crystalline structure of the corresponding composition does not involve phosphate chain length growth. The latter comparison suggests that the state of polymerization in both the crystal and glass phosphate backbone of similar composition is insensitive to hydrostatic pressure. Based on this hypothesis, the crystalline form of zinc orthophosphate was pressurized. In accordance with the pyrophosphate results, changes in the Raman spectra of the zinc orthophosphate do not show evidence for polymerization of phosphate compounds when pressurized up to 20.7 GPa.

When subjected to high pressure, short-chain zinc pyro- and ortho-phosphate do not polymerize whether they are in the glassy or crystalline form. Stresses existing at very high pressures involve some loss of order in the crystalline sample structure.[27,28] One may argue that the apparition of nonhydrostaticity at very high pressure in the sample chamber could prevent the observation of a polymerization in phosphate chains. However, in reality, tribofilm pressures are far from perfectly hydrostatic, and yet we observe long-chain zinc phosphates. As a consequence, the loss of order in the structure of our sample should not compete with polymerization of phosphate chains.

Mosey *et al.*[11] have reported the role of zinc as a cross-linking agent by increasing its coordination number in pressurized zinc phosphates. In this study, Raman spectroscopy is not suited to probe Zn-O ionic bonds in zinc phosphate materials. Thus, we cannot probe the coordination of zinc as the pressure increases. However, vibrational properties of the PO_4 tetrahedron are sensitive to the immediate environment of the cation. Hence, the tremendous modifications appearing in the Raman spectra observed for zinc orthophosphate at a few GPa could be interpreted in terms of zinc coordination changes with pressure. This hypothesis must be clarified, so EXAFS experiments are planned in order to highlight the zinc coordination when zinc phosphate materials experience high pressure.

V. CONCLUSION

In this study, *in situ* Raman spectroscopy was performed on zinc ortho- and pyro-phosphate loaded in a diamond anvil cell up to 20 GPa. The diamond anvil cell simulates flash pressure experienced on the top of tribofilm pads and uncouples the effect of pure pressure from friction in a tribological contact. Using *in situ* Raman spectroscopy, we probe the state of polymerization of phosphate compounds in zinc phosphate samples as the pressure increases. This experimental setup is designed to evaluate the role of pressure in extending phosphate chain lengths as supposed by previous studies of the ZDTP tribofilm. At very high pressure the samples undergo irreversible loss of order in the initial structure confirmed by broadening of the Raman bands of resonance. This study demonstrates that pressure-induced structural modifications in the phosphate backbone does not affect the degree of polymerization of phosphate chains.

ACKNOWLEDGMENTS

The authors thank Budenheim and Brentag companies for providing the zinc pyrophosphate sample. This work was supported by the Région Rhone-Alpes.

[1] H. Spikes, Tribol. Lett. **17**, 469 (2004).
[2] K. Topolovec-Mikložič and H. A. Spikes, J. Tribol. **127**, 405 (2005).
[3] K. Demmou *et al.*, Tribol. Int. **39**, 1558 (2006).
[4] M. A. Nicholls *et al.*, Tribol. Lett. **15**, 241 (2003).
[5] M. Eglin, A. Rossi, and N. D. Spencer, Tribol. Lett. **15**, 199 (2003).
[6] C. Minfray *et al.*, Tribol. Lett. **21**, 65 (2006).
[7] Z. Zhang *et al.*, Tribol. Lett. **19**, 221 (2005).
[8] J. M. Martin *et al.*, Tribol. Int. **34**, 523 (2001).
[9] J. M. Martin *et al.*, ASLE Trans. **29**, 523 (1985).
[10] M. A. Nicholls *et al.*, Tribol. Lett. **17**, 205 (2004).
[11] N. J. Mosey, M. H. Müser, and T. K. Woo, Science **307**, 1612 (2005).
[12] N. J. Mosey and T. K. Woo, Inorg. Chem. **45**, 7464 (2006).
[13] J. F. Graham, C. McCague, and P. R. Norton, Tribol. Lett. **6**, 149 (1999).
[14] R. K. Brow *et al.*, J. Non-Cryst. Solids **191**, 45 (1995).
[15] R. K. Brow, J. Non-Cryst. Solids **263–264**, 1 (2000).
[16] K. Meyer, J. Non-Cryst. Solids **209**, 227 (1997).
[17] B. C. Tischendorf *et al.*, J. Non-Cryst. Solids **282**, 147 (2001).
[18] H. J. de Jager and L. Prinsloo, Thermochim. Acta **376**, 187 (2001).
[19] B. Mysen, Am. Mineral. **81**, 1531 (1996).
[20] M.J. Toplis and B. Reynard, J. Non-Cryst. Solids **263–264**, 123 (2000).
[21] G. T. Stranford and R. A. Condrate, J. Mol. Struct. **73**, 231 (1981).
[22] R. L. Frost, Spectrochim. Acta, Part A **60**, 1439 (2004).
[23] Natl. Bur. Stand. (U.S.), Monogr. 25, 80 (1979).
[24] T. Bataille, P. Bénard-Rocherull, and D. Louër, J. Solid State Chem. **140**, 62 (1998).
[25] H. K. Mao, J. Xu, and P. M. Bell, J. Geophys. Res. **91**, 4673 (1986).
[26] M. Miyamoto *et al.*, Mineral. J. **16**, 246 (1993).
[27] P. Gillet *et al.*, Phys. Rev. B **51**, 11262 (1995).
[28] D. Machon *et al.*, J. Phys. Condens. Matter **18**, 3443 (2006).
[29] M. J. Peters, M. Grimsditch, and A. Polian, Solid State Commun. **114**, 335 (2000).